Reactivity, Formation, and Solubility of Polyoxometalates Probed by Calorimetry

Hrafn Traustason,[†] Nicola L. Bell,[‡] Kiana Caranto,[§] David C. Auld,[‡] David T. Lockey,[‡] Alex Kokot,[§] Jennifer E.S. Szymanowski,[§] Leroy Cronin,[‡] Peter C. Burns*[,†,§]

[†]Department of Chemistry and Biochemistry, University of Notre Dame, Notre Dame, Indiana 46556, United States
[‡]School of Chemistry, University of Glasgow, University Avenue, Glasgow, G12 8QQ, UK
[§]Department of Civil & Environmental Engineering & Earth Sciences, University of Notre Dame, Notre Dame, Indiana 46556, United States

Correspondence: pburns@nd.edu

Abstract

Room temperature calorimetry methods were developed to describe the energy landscapes of six polyoxometalates (POMs), Li–U_{24}, Li–U_{28}, K–U_{28}, Li/K–U_{60}, Mo_{132}, and Mo_{154}, in terms of three components: enthalpy of dissolution (ΔH_{diss}), enthalpy of formation of aqueous POMs ($\Delta H_{f,(aq)}$), and enthalpy of formation of POM crystals ($\Delta H_{f,(c)}$). ΔH_{diss} is controlled by a combination of cation solvation enthalpy and the favorability of cation interactions with binding sites on the POM. In the case of the four uranyl peroxide POMs studied, clusters with hydroxide bridges have lower $\Delta H_{f,(aq)}$ and are more stable than those containing only peroxide bridges. In general for POMs, the combination of calorimetric results and synthetic observations suggest that spherical topologies may be more stable than wheel-like clusters, and $\Delta H_{f,(aq)}$ can be accurately estimated using only $\Delta H_{f,(c)}$ values owing to the dominance of the clusters in determining the energetics of POM crystals.

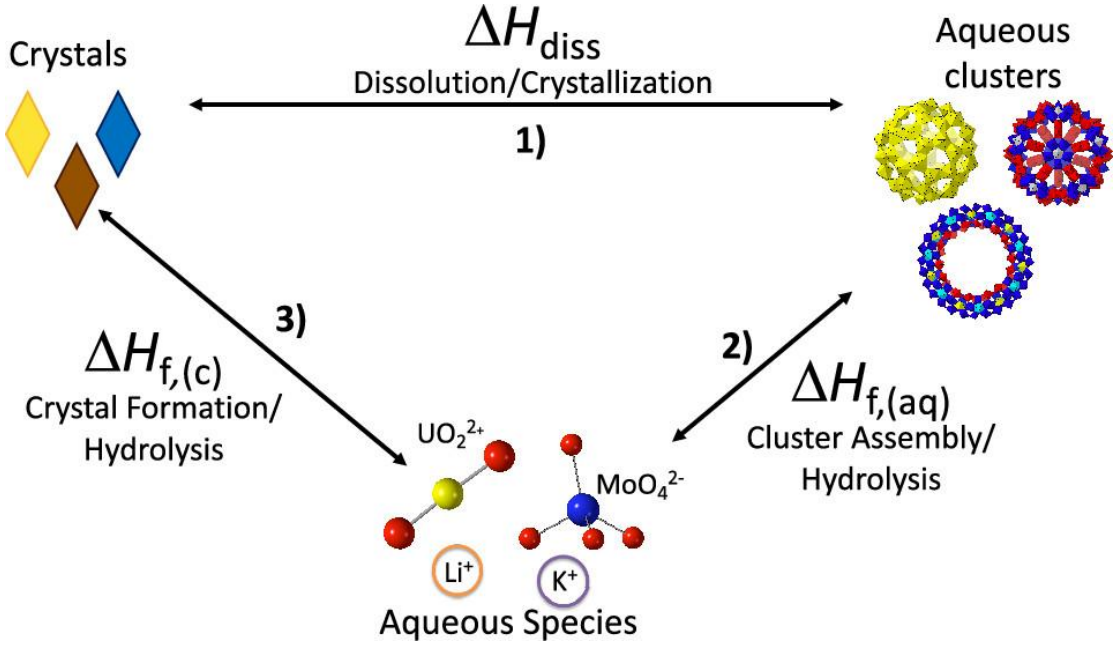

Introduction

Polyoxometalates (POMs) are a family of discrete molecular metal-oxide anionic clusters consisting of transition and/or actinide metals in high oxidation states (typically V/VI).(1) They are known for their formation by self-assembly, structural diversity, as well as their wide-ranging potential and realized applications including but not limited to catalysis,(2) sustainable energy,(3) electronics,(4) and sensors.(5) Relatively recently discovered actinide POMs also have potential applications in recycling nuclear fuels(6,7) and fabrication of mixed oxide fuels.(8) POMs are valuable models for studying structure-size-property relations such as aggregation behavior in solution because they are larger than most inorganic complexes but smaller than colloids and are dissolvable as macroanions in various solvents.(9) Geochemically important POMs have been preserved in 42 POM minerals(10,11) and are likely important in metal transport in various geochemical and environmental systems.(12) Despite the wide-ranging aforementioned significance of POMs extending from basic scientific interest to sustainable energy applications, little is known about their thermodynamics and stabilities in various systems.

The structural and compositional diversity of POMs has grown substantially in the last two decades through efforts in direct synthesis.(13,14) The final composition and topology of a POM can be influenced by small changes in pH, ionic strength, counterions, and reaction temperature,(13,15) and it is often difficult to distinguish kinetically favored POMs from those that are stable. Although most POMs are produced via de-novo "one-pot" syntheses, some POMs have only been synthesized by derivation from other more readily accessible POMs via ligand or metal substitution, resulting in altered structures and properties.(16) Great emphasis has been placed on understanding the solution behavior of POMs with special attention to formation mechanisms,(17−21) the role of counter cations,(22,23) crystallization,(24) solubility,(25,26) and transformations.(27) It has recently been suggested that counter cations can dramatically affect the conformation and reactivity of POMs in solution,(27) in addition to balancing their charge and mediating aggregation and crystallization.

Subfamilies of POMs have emerged that include the actinyl peroxides, molybdenum browns and molybdenum blues.(15) The actinyl peroxide clusters were first reported in 2005 and include uranyl (UO_2^{2+}) or neptunyl ($NpO_2^{1+/2+}$) based clusters in which actinyl ions are bridged by peroxo ligands into cages.(28) This family includes more than 60 uranyl peroxide clusters (UPCs) containing anywhere from 16–124 U atoms and provides a unique vehicle for studying the actinide elements.(14) Despite the extensive library of topologically unique UPCs, solution characterization studies have shown that four clusters (U_{20}, U_{24}, U_{28}, and U_{60}) are dominant in reaction solutions over a broad range of conditions.(29,30) Their formation and crystallization can be impacted by adjustment of counter cations although the details remain unclear.(15)

Descriptions of the thermodynamic properties of polyoxometalate systems are generally absent from the literature, although considerable insight could result from detailed studies of selected systems. Careful measurements of properties such as enthalpies of cluster formation, and of crystallization/dissolution of cluster salts would provide useful insights into the thermodynamic stability and formation mechanisms of polyoxometalates, as well as factors governing their solution behavior. We are particularly interested in better understanding the role of thermodynamics in influencing different topological arrangements of uranyl ions in

UPCs, as well as the interaction of counter cations with clusters more generally. For example, the U_{60} cluster contains 60 uranyl ions arranged in a fullerene topology that is identical to that of C_{60}.(31) There are 1812 fullerene topologies with 60 vertices. Whereas in the case of C_{60} the avoidance of pentagonal adjacencies favors this topology, which is the only 60-vertex fullerene with no adjacent pentagons and also the highest symmetry, it remains unclear why the topology is also common in the uranyl peroxide system.(31)

Here we have developed new methodologies for the study of the thermodynamic parameters of POM formation based upon existing calorimetric instrumentation, with an emphasis on UPCs and selected Mo based POMs. Previous calorimetric measurements addressed the enthalpies of formation of selected salts of UPCs(32–34) but did not disentangle the energetics of self-assembly of clusters in solution and their later crystallization. As such, it is impossible to discern, for example, the energetics of assembly of uranyl ions to form the cluster, the interactions of counter cations with the cluster, and the energetics of the linkages of clusters that occur through counter cations and H_2O groups during crystallization. Six POMs have been selected for study here: Li–U_{24}, Li–U_{28}, K–U_{28}, Li/K–U_{60}, Mo_{132}, and Mo_{154} (full chemical formulae are available in Table S6 thermochemical cycles). Polyhedral representations of each are shown in Figure 1. In the case of the uranyl peroxide cage clusters U_{24}, U_{28}, and U_{60}, the counter cations present in the salt are Li or K or both, and for Mo_{132} and Mo_{154}, NH_4 and Na are present, respectively. These POMs were selected because they have been extensively studied as reported in the literature(15,35) and are the most prevalent POMs detected under various synthetic conditions.(29)

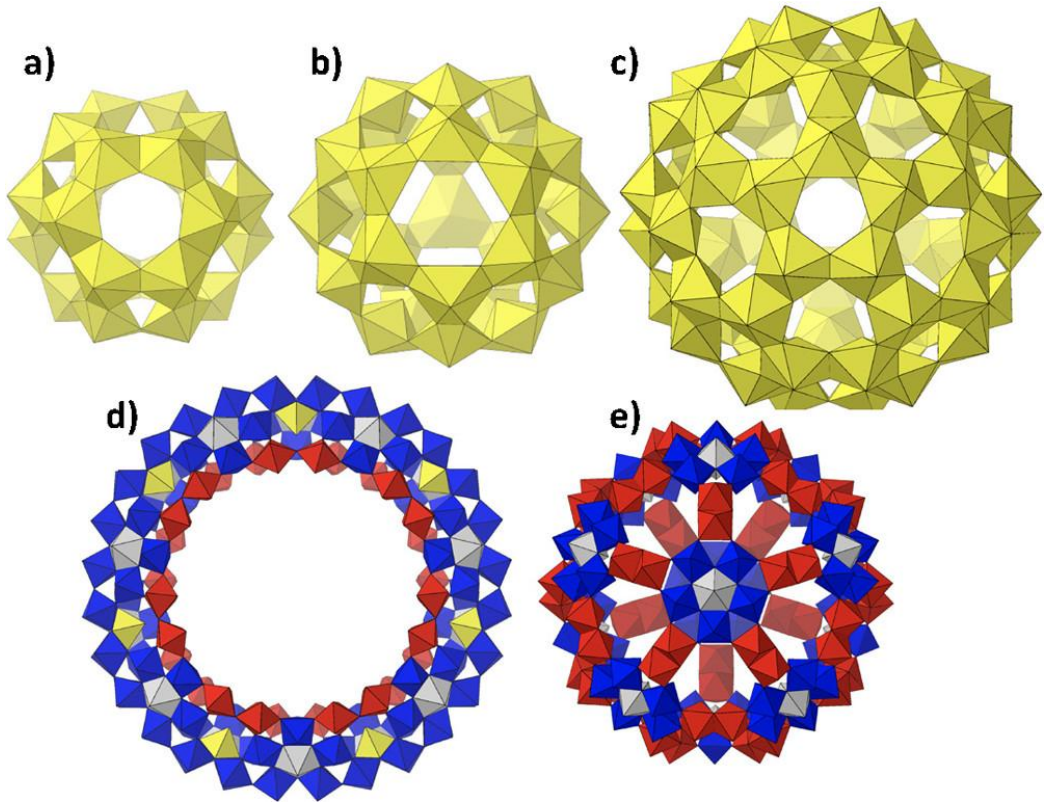

Figure 1. POMs of interest: (a) U24, (b) U28, (c) U60, (d) Mo154, and (e) Mo132. Uranyl polyhedra are shown in yellow in panels a–c. Panels d and e demonstrate four different Mo building blocks: {Mo1} in yellow, {Mo2} in red, {Mo6} in dark blue and silver, and {Mo8} in blue and silver.

Methods

Caution: The uranium used in these experiments, although isotopically depleted, is radioactive and should only be handled by trained individuals in appropriate facilities.

Synthesis and Characterization

Salts of the POMs selected for study here were synthesized according to literature methods(28,32,36−38) with modifications detailed in the Supporting Information. Prior to calorimetric measurements, materials were extensively characterized by single-crystal X-ray diffraction (SCXRD) and thermogravimetric analysis (TGA). Solutions produced by dissolving the various cluster compounds were analyzed by inductively coupled plasma optical emission spectroscopy (ICP-OES) and electrospray ionization mass spectroscopy (ESI-MS). Although powder X-ray diffraction is often used to verify purity of crystalline solids, it is not useful in the current case because crystals of UPCs degrade during grinding and their very large unit cells and elaborate structures result in complex patterns in which the presence of impurities could easily be overlooked. Details of each method and results are provided in the Supporting Information.

Calorimetric Measurements

Characterization of the enthalpic landscape of metal oxide clusters requires determination of (1) the enthalpy of dissolution of salts of the POMs into water (ΔH_{diss}) (equal but opposite the enthalpy of crystallization) without destruction of the POMs, (2) the enthalpy of formation of the POMs in water from their basic constituents ($\Delta H_{f,(aq)}$), and (3) the enthalpy of formation of POM crystals ($\Delta H_{f,(c)}$) that includes both the enthalpy of POM assembly and its crystallization (Figure 2). Calorimetric measurements of the data needed to derive ΔH_{diss}, $\Delta H_{f,(aq)}$, and $\Delta H_{f,(c)}$ were performed for aqueous solutions of the clusters at room temperature using a Setaram C-80 mixing calorimeter. To do so, known quantities of reactants were placed in the calorimeter that was allowed to thermally stabilize prior to mixing and measurement of the enthalpy of the reaction of interest. Further details of this method, including the sample vessels, is in the Supporting Information.

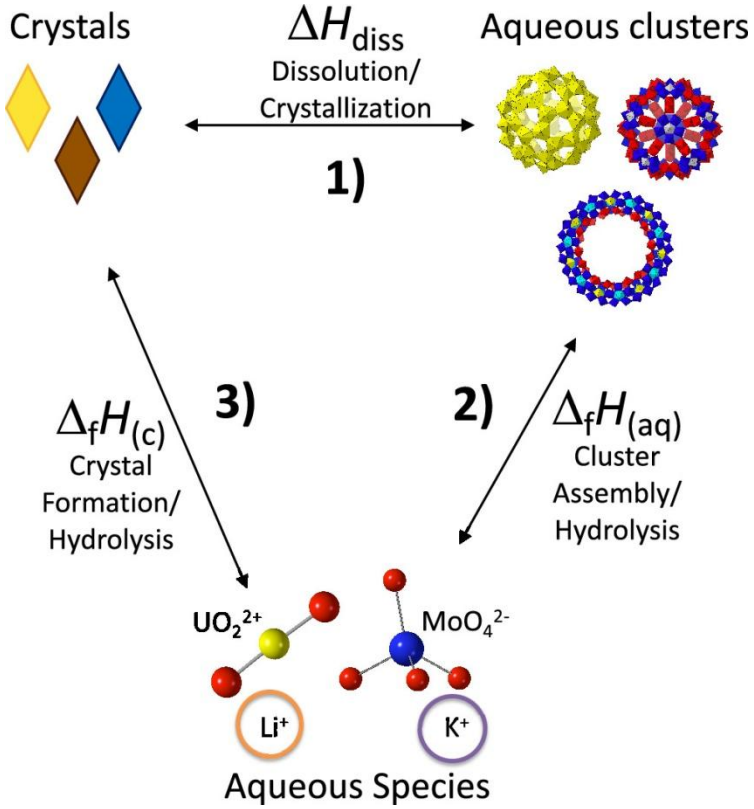

Figure 2. Schematic of the three measurements needed to define the energy landscape of the POMs.

For each of the six compounds under study, three calorimetric measurements were made at room temperature (specifics are given here for Li–U_{24}, all reactions are documented in Table S6, Supporting Information): (1) the heat of dissolution of POM salts into water to directly measure ΔH_{diss} (reaction R1), (2) the heat of mixing of aqueous solution containing POMs with appropriate acidic (6 M HCl) or basic (4 M NaOH) solutions that trigger breakdown of the POMs to simple aqueous species (reaction R2; UO_2^{2+}, Li^+, K^+, MoO_4^{2-}, etc.)(39) and the resulting heat was used to calculate $\Delta H_{f,(aq)}$, and (3) the heat of dissolution of POM crystal salts into an acidic or basic solution suitable to both dissolve the solid and destroy the POM and the measured heat of the reaction (reaction R3) was used to calculate $\Delta H_{f,(c)}$. The sum of $\Delta H_{f,(c)}$ and ΔH_{diss} corresponds to the summation of $\Delta H_{f,(aq)}$ and the standard formation enthalpy of all lattice waters in the POM structure as shown in eq 1. Details of the calorimetric measurements are provided in the Supporting Information. Thermochemical cycles were used to derive the formation enthalpies of the POMs from their elements under standard conditions and are given in Table S6.

$$Li_{24}[UO_2O_2OH]_{24}\cdot 83H_2O_{(c)} + n\,H_2O_{(l)} \rightarrow Li_{24}[UO_2O_2OH]_{24(aq)} + (n+83)H_2O_{(l)}$$

(R1)

$$Li_{24}[UO_2O_2OH]_{24(aq)} + 72HCl_{(aq)} \rightarrow 24Li^+_{(aq)} + 24UO^{2+}_{2(aq)} + 48H_2O_{(l)} + 12O_{2(g)} + 72Cl^-_{(aq)}$$

(R2)

$$Li_{24}[UO_2O_2OH]_{24}\cdot 83H_2O_{(c)} + 72HCl_{(aq)} \rightarrow 24Li^+_{(aq)} + 24UO^{2+}_{2(aq)} + 131H_2O_{(l)} + 12O_{2(g)} + 72Cl^-_{(aq)}$$

(R3)

$$\Delta H^\circ_{f,(c)} \xrightarrow{\Delta H_{diss}} \Delta H^\circ_{f,(aq)} + n\Delta H^\circ_f(H_2O)$$

(1)

Data for calculation of $\Delta H_{f,(c)}$ was also derived for crystals of each POM under study (except Mo_{132} owing to the presence of organic components) from measurements of the enthalpy of dissolution of the material into a sodium molybdate solvent at 700 °C in a Calvet-type Setaram AlexSys high-temperature oxide melt drop solution calorimeter (reaction R4). This high-temperature calorimetry method is well established for measurements of enthalpies of dissolution of uranyl compounds including POMs.(32−34,40) Pellets of 5–10 mg of sample were pressed and dropped from room temperature into sodium molybdate solvent at 700°C resulting in the sample dissolving and cluster breakdown. The calorimeter was calibrated using the heat content of α-Al_2O_3. During measurements O_2 was flushed through the calorimeter to sweep away any evolved gases and also bubbled into the solvent to ensure oxidizing conditions and dissolution of the metal cations in their highest oxidation states.

$$Li_{24}[UO_2O_2OH]_{24}\cdot 83H_2O_{(c)} \rightarrow 12Li_2O_{(sln,700\ ^\circ C)} + 24UO_{3(sln,700\ ^\circ C)} + 12O_{2(g,700\ ^\circ C)} + 95H_2O_{(g,700\ ^\circ C)}$$

(R4)

Results and Discussion

The salts of the six POMs under study were synthesized in their pure forms by literature methods and analyzed by TGA to determine hydration levels (see the Supporting Information S3). Calorimetric measurements proved to be relatively straightforward and problem free, although the room temperature measurements consumed significant time because of the slow return to calorimeter baseline. The calorimetry methodology used here is broadly suitable for studies of the enthalpies of reactions involving POMs and other metal-oxide clusters, including formation and dissolution into solvents. We selected POMs for study that are highly soluble in water and that rapidly decompose when conditions become acidic (uranyl peroxide clusters) or basic (Mo POMs). Calorimetric measurements in POM-bearing systems are only useful if the starting and end points are clearly defined. In the current study, the starting point was either the crystallized form of the POM that was characterized by X-ray diffraction and other methods in earlier studies, or the POM dissolved intact in an aqueous solution, which was confirmed using mass spectrometry. The end points were either POMs dissolved in aqueous solution, confirmed by mass spectrometry, cluster breakdown products in solution, confirmed by mass spectrometry, or cluster breakdown products dissolved in a sodium molybdate solvent at 700 °C. It is also important to select conditions under which the aqueous species are unambiguous, such as for uranyl in acidic conditions. Subsequent to the room-temperature calorimetry, visual inspection of the resulting final state indicated that there was no precipitate. For the high-temperature calorimetry, preliminary tests of sample solubility in sodium molybdate solvent at 700 °C were done for solvent contained in a crucible in a furnace.(41)

Enthalpy of Formation of POM Crystals

Calorimetric measurements to determine the enthalpy of formation of POM crystals ($\Delta H_f^\circ{}_{(c)}$,Figure 2) of UPCs and Mo based POMs were conducted in a C-80 mixing calorimeter using 6 M HCl and 4 M NaOH, respectively, to ensure full breakdown of the cluster into simple species as verified by ESI-MS. The resulting $\Delta H_f^\circ{}_{(c)}$ values for Li–U_{24}, Li–U_{28}, and Li/K–U_{60} are in good agreement with values that were measured

using high temperature drop solution calorimetry (Table 1), confirming that the experimental set up and method development for the C-80 was successful.(32,34) The value for K–U_{28} is only in fair agreement (9.15%) with the high-temperature calorimetry-derived values. This may be due to the lengthy time required for the calorimeter to return to baseline after reacting K–U_{28} samples with 6 M HCl.

Table 1. ΔHf°(c) Values from Previously Published Papers[a] and C-80 Room Temperature Calorimetry Results[b]

cluster	AlexSys $\Delta H_f°_{(c)}$ (kJ/mol)	adjusted $\Delta H_f°_{(c)}$ (kJ/mol)	C-80 $\Delta H_f°_{(c)}$ (kJ/mol)	discrepancy
Li–U_{24}	–66 323.51 ± 315.4	–66 323.51 ± 315.4	–63 584.39 ± 264.8	4.31%
Li–U_{28}	–65 425.13 ± 119.09	–66 854.13 ± 119.09	–63 841.72 ± 20.3	4.72%
K–U_{28}	–57 546.56 ± 185.72	–56 689.16 ± 185.72	–51 936.43 ± 406.9	9.15%
U_{60}	–167 060 ± 310	–170 780 ± 310	–166 809.6 ± 34.1	2.38%

[a] The thermodynamic cycles used to calculate the enthalpies of formation of these compounds from the calorimetric data are significantly impacted by the number of water groups per formula unit. Determination of water contents via thermogravimetric analysis is complicated by the presence of peroxide and hydroxyl, as detailed in the Supporting Information. The enthalpies of formation of Li–U_{28}, K–U_{28}, and U_{60} from the original reports have been adjusted for water contents consistent with the approach detailed in the Supporting Information.
[b] Values for Li–U_{28} and K–U_{28} are from Sharifironizi et al.(32) and U_{60} values are from Armstrong et al.(34)

Enthalpy of POM Dissolution and Crystallization

It is well known that various types of POMs, including the Mo based POMs and UPCs studied here, self-assemble in solution prior to crystallization, and that upon dissolution of salts of these POMs, the clusters can persist indefinitely in solution.(15,42,43) Owing to the presence of strong metal–oxygen bonds, the enthalpies of formation of the POM clusters are expected to be larger than the enthalpy of crystallization of the clusters, although this has not been previously quantified. The enthalpy of self-assembly of the individual POMs from simpler species in solution is independent of the crystallization process, but both are captured by measuring the enthalpy of formation of POM crystals by reacting POM crystals with either basic or acidic water at room temperature or by dissolution in a solvent at high temperature. The enthalpy of dissolution (ΔH_{diss}, Figure 2) of salts of POMs is the heat of dissolving crystals containing POMs into a solution in which the POMs remain intact (n.b. the heat of crystallization is the opposite of this value). The ΔH_{diss} measured for all six POMs under study here are very small and positive (Table 2), indicating that dissolution is entropically driven and that the enthalpy of formation of a POM crystal is mostly attributable to the formation of the POM itself. Entropy of dissolution (ΔS_{diss}) is positive when transitioning from clusters ordered in a single crystal to those free to diffuse in an aqueous solution.

Table 2. ΔHdiss, ΔHf°(aq), and ΔHf°(c) Normalized to One U/Mo (ΔHdiss/M, ΔHf°(aq)/M, and ΔHf°(c)/M)a

cluster	$\Delta H_{diss}/M$ (kJ/mol)	$\Delta H_f°_{(aq)}/M$ (kJ/mol)	$\Delta H_f°_{(c)}/M$ (kJ/mol)
Li–U_{24}	3.43 ± 0.56	–1849.1 ± 0.4	–2649.3 ± 11.0
			–2763.5 ± 13.1*
Li–U_{28}	0.35 ± 0.05	–1706.0 ± 0.6	–2280.1 ± 0.7
K–U_{28}	5.23 ± 0.75	–1683.3 ± 0.1	–1854.9 ± 14.5
U_{60}	3.05 ± 0.03	–1852.1 ± 0.5	–2780.2 ± 0.6
Mo_{132}	6.09 ± 0.78	–1040.3 ± 10.8	–1776.7 ± 3.9
Mo_{154}	0.96 ± 0.05	–922.4 ± 0.5	–1701.7 ± 28.4*

[a] Values labelled with an asterisk (*) were measured using an AlexSys calorimeter.

Computational studies indicate that alkali metal cations have affinity for specific binding sites corresponding to topological windows in UPCs, with interaction of Li with square windows and K with pentagonal windows preferred.(44) Also, Li has a double hydration sphere in aqueous solution and a high enthalpy of hydration.(44,45) As such, we propose that there are two processes that are dominant in ΔH_{diss} (Figure 3): (i) the detachment of counter cations from the cage (unfavorable) and (ii) and the solvation of counter cations by water molecules (favorable). As such, the range of measured ΔH_{diss} over the six POMs under study is consistent with the presence of different counter cations and the differing charge densities of the UPCs.(32)

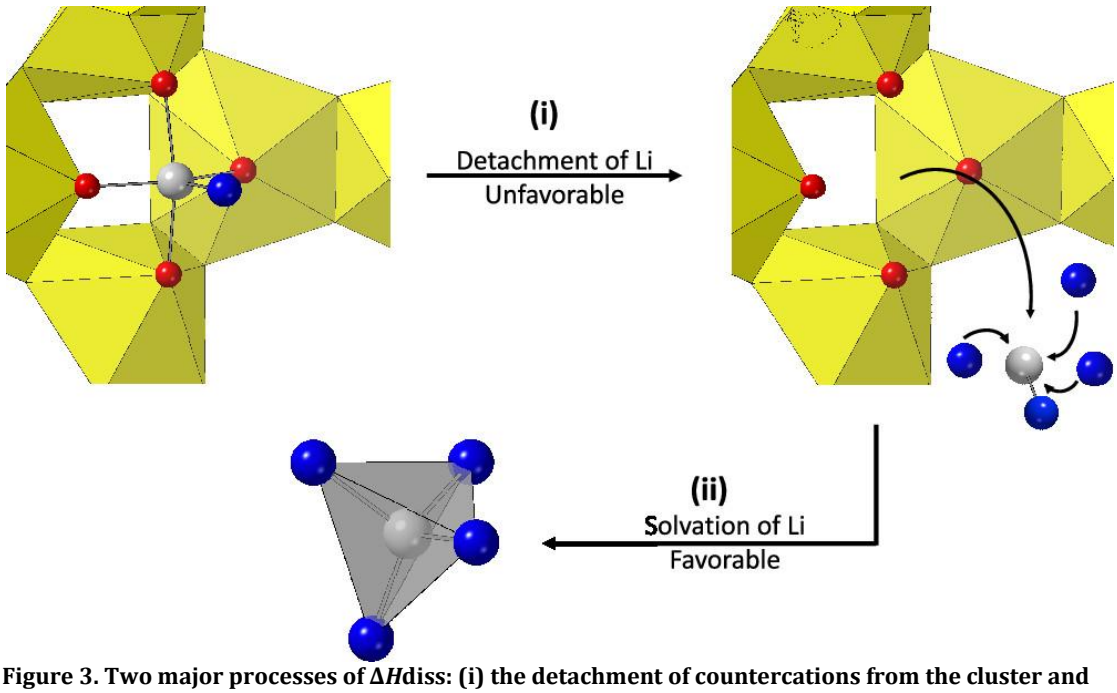

Figure 3. Two major processes of Δ*H*diss: (i) the detachment of countercations from the cluster and (ii) the solvation of countercations. Uranyl polyhedra are shown in yellow, oxygen atoms attached to the cage are shown in red, water oxygens in blue, and Li in silver.

Upon normalization of the ΔH_{diss} for UPCs to the number of moles of uranium ($\Delta H_{diss}/M$), the values fall in the order of K–U_{28} > Li–U_{24} > Li/K–U_{60} > Li–U_{28}. Consider first the two salts of U_{28}, as the clusters in these are chemically and topologically identical and have the same negative charge density. The observed values of ΔH_{diss} are consistent with the presence of pentagonal and hexagonal windows only (See Table S1), which provide good sites for bonding K, and the more favorable solvation enthalpy of Li as compared to K.(44) In the case of Li–U_{24} and Li/K–U_{60}, the topology of the cages includes the preferred windows of their respective counter cations and hence, they have similar ΔH_{diss}.

The $\Delta H_{diss}/M$ normalized to moles of molybdenum for Mo_{132} and Mo_{154} are 6.09 and 0.96 kJ/mol, respectively, with that of Mo_{132} the highest amongst the POMs studied here. Mo_{132} is charge balanced by NH_4^+ cations, and enthalpies of dissolution for ammonium salts are generally highly endothermic because water molecules bind to ammonium cations via hydrogen bonds and hence not as strongly as they do for alkali metals through dative bonding.(46,47) The measured $\Delta H_{diss}/M$ of Mo_{154} is the second lowest of the POMs studied here, perhaps because Mo_{154} has considerably fewer counter cations per metal and a corresponding lower charge density (15:153, see the Supporting Information) than any of the other POMs under study.

The enthalpy of crystallization (ΔH_{cryst}) and entropy of crystallization (ΔS_{cryst}) are equal but opposite to ΔH_{diss} and ΔS_{diss}, respectively. Since ΔH_{cryst} is only slightly favorable and ΔS_{cryst} must be unfavorable, the entropy change at room temperature must be smaller than the change in enthalpy ($|\Delta H_{cryst}| > |T\Delta S_{cryst}|$) for the overall crystallization process to be favorable ($\Delta G_{cryst} < 0$). The very low ΔH_{cryst} for these clusters is consistent with the remarkably high solubility of many of the POMs, including UPCs that can reach U concentrations as high as 1.8 M when dissolved in pure water and >2 M for molybdenum POMs in acidic media.(29) Experimental and computational studies have established that U_{60} crystallization occurs from a solution containing an approximately close-packed array of clusters,(25) which is a more ordered solution state than typical and consistent with only a small change of entropy during the crystallization process. Similarly, Mo based POMs are known to form extended "blackberry" structures in solution, increasing the degree of long-range order of these clusters in solution.(48)

Enthalpy of Formation of Aqueous POMs

The enthalpy of formation of aqueous POMs ($\Delta H_f°_{(aq)}$, Figure 2.2) for Li–U_{24}, Li–U_{28}, K–U_{28}, Li/K–U_{60}, Mo_{132}, and Mo_{154} were determined with good precision and are shown in Table 2 as $\Delta H_f°_{(aq)}$ normalized to one mole of metal (M). The formation enthalpies for the aqueous POMs are highly favorable, consistent with their rapid self-assembly in solution. Two of the UPC clusters have both hydroxo and peroxo bridges between uranyl ions (U_{24} and U_{60}), and these have significantly larger enthalpies of formation than those with only peroxo bridges between uranyl ions (U_{28}). It is possible that the hydroxo bridges are stabilizing in the topologies of UPCs.(30) In an earlier study, small angle X-ray scattering (SAXS) data indicated a transition from U_{28} to U_{24} during solution aging (reaction R5).(30) Our current results suggest that U_{28} may be kinetically favored, whilst U_{24} is thermodynamically preferred, although it is important to note that the quantity of unbound peroxide in solution decreases with time due to its breakdown and this may favor clusters with fewer peroxide bridges. The thermodynamic values obtained here allow us to calculate the enthalpy of reaction ($\Delta H_{rxn}/M$) for the transformation of Li–U_{28} to Li–U_{24} (eq 2): −133.3 kJ/mol and demonstrate that this transformation is highly favorable.

$$6Li_{28}[UO_2(O_2)_{1.5}]_{28(aq)} + 12H_2O_{(l)} \rightarrow 7Li_{24}[UO_2O_2OH]_{24(aq)} + 6O_{2(g)} \quad \text{(R5)}$$

$$\Delta H_{rxn} = 7\Delta H_f^\circ(Li - U_{24(aq)}) + 6\Delta H_f^\circ(O_{2(g)}) - (6\Delta H_f^\circ(Li - U_{28(aq)}) + 12\Delta H_f^\circ(H_2O_{(l)}) \quad \text{(2)}$$

The $\Delta H_f°_{(aq)}$ values for molybdenum POMs demonstrate the higher stability of Mo_{132} (−1041.1 kJ/mol) cf. Mo_{154} (−981.5 kJ/mol). This corresponds well to the synthetic observation that facile transformation of Mo_{154} into Mo_{132} occurs upon treatment with excess reducing agent. In contrast the corresponding oxidation of Mo_{132} yielded only the spherical Mo_{102} rather than the molybdenum wheel framework (See SI, section 1). The increased stability of Mo_{132} may arise from the presence of a reduced edge-sharing (2 × {κ^2-O}) Mo_2 unit, containing an Mo–Mo bond, rather than a corner-sharing ({κ^2-O}) dimer and from the spherical topology rather than the wheel-like Mo_{154} framework.

Breakdown reactions of some of the studied POMs in solution at room temperature were slow (10–12 h) thus we consider high temperature calorimetry to be more suitable to derive the enthalpy of formation of POM crystals. The $\Delta H_f°_{(c)}$ in

combination with $\Delta H_{(diss)}$ yields $\Delta H_f°_{(aq)}$ (eq 1) and these values are in good agreement with the measured $\Delta H_f°_{(aq)}$ (Table 3) when using values derived from high-temperature calorimetry. One can obtain reliable estimates of $\Delta H_f°_{(aq)}$ having only $\Delta H_f°_{(c)}$ values because ΔH_{diss} is insignificant in comparison to $\Delta H_f°_{(aq)}$ and the standard formation enthalpy of H_2O is constant.

Table 3. Calculated Values for Δf°H(aq) Using Δf°H© from High-Temperature Calorimetry Are in Good Agreement with the Measured Values Demonstrating That One Could Calculate Reliable ΔHf°(aq) Values by Using Only ΔHf°(c)a

POM	$\Delta H_f^\circ{}_{(aq)}/M$ – calculated (kJ/mol)	$\Delta H_f^\circ{}_{(aq)}/M$ – measured (kJ/mol)	discrepancy
$Li–U_{24}$	–1771.7 ± 13.1	–1849.1 ± 0.4	4.19%
$Li–U_{28}$	–1642.2 ± 4.3	–1706.0 ± 0.6	3.74%
$K–U_{28}$	–1606.0 ± 6.6	–1683.3 ± 0.1	4.59%
U_{60}	–1761.9 ± 5.1	–1852.1 ± 0.5	4.87%
Mo_{154}	–983.5 ± 28.4	–922.4 ± 0.4	6.62%
Mo_{132}	–1041.4 ± 3.9*	–1040.1 ± 10.8	0.13%

[a] The $\Delta_f°H_{(c)}$ used to calculate values for $\Delta_f°H_{(aq)}$ marked with an asterix (*) could not be measured using high-temperature calorimetry due to its organic components.

Conclusion

We have developed calorimetric methods that yield thermodynamic values never before measured for POMs ($\Delta H_f^\circ{}_{(aq)}$ and ΔH_{diss}). The methods for room temperature calorimetry yielded good agreement with values obtained by high temperature drop solution calorimetry that has been used for decades, although we consider the high temperature drop solution calorimetry method more suitable when measuring POMs in crystal form because the dissolution reaction occurs quickly.(32,34)
The POMs under study here are inherently nanoscale materials that are stabilized in aqueous solution by the presence of multiply bonded oxygen atoms on their surfaces. The broad range of potential applications of POMs, as well as their importance in geochemical and environmental systems, arise from their often exceptionally high solubility in aqueous solutions. The POMs are macroanions in aqueous solution that have associated counter cations that in some cases occur in cavities within the POM, and the overall charge of the POM-counter cation assemblage depends on POM size and identity, solution pH, and POM concentration.(48) The findings here that the enthalpies of dissolution of POM crystals are very small and positive is consistent with the entropically driven dissolution process and high aqueous solubility of the POMs.
In the case of the UPCs, the enthalpies of formation of clusters with both peroxo and hydroxo bridges between uranyl ions are more negative than those of UPCs containing only peroxo bridges, consistent with experimental observations that revealed formation of U_{28} (peroxo bridges only) initially in alkaline aqueous solution followed by gradual replacement by U_{24} (both peroxo and hydroxo bridges).(30) Hypothetically, combining uranyl-peroxo-uranyl bridges that typically have strongly bent dihedral angles with uranyl-hydroxo-uranyl bridges that can have flatter dihedral angles may result in a more stable cage. However, the presence of topological squares (tetramers) in UPCs can only occur when some of the uranyl bridges are not peroxo, and the presence of topological squares, pentagons, and hexagons in UPCs provide a variety of cation binding sites that may impact stability in complex ways. Both the U_{32R} and U_{28} clusters occur with exclusively peroxo bridges and also with combinations of peroxo and hydroxo bridges, which may provide an opportunity in the future for gaining more insight into the stability implications of incorporation of these two types of bridges.(49−51)
For Mo based POMs the spherical Keplerate Mo_{132} was found to be more stable than ring-shaped Mo_{154} consistent with synthetic observations that while Mo_{154} can be transformed into Mo_{132} by reduction, oxidation of Mo_{132} yields only spherical Mo_{102}, suggesting spherical topologies may be inherently more stable than others. The calculated enthalpy of POM crystals for all POMs studied is in good agreement with the measured value when using $\Delta H_f^\circ{}_{(c)}$ obtained by high temperature calorimetry and hence supports our interpretation of the energy landscape of the clusters. ΔH_{diss} is negligible in the calculations of $\Delta H_f^\circ{}_{(aq)}$ and therefore one can obtain reasonably predictive values of $\Delta H_f^\circ{}_{(aq)}$ of POMs from $\Delta H_f^\circ{}_{(c)}$ values.
Our methods can be adapted to accommodate different subfamilies of POMs as demonstrated with UPCs and the Mo based POMs studied here. Thermodynamic studies may enhance our understanding of reactions, assembly, and crystallizations of POMs and it is our hope that the experimental thermodynamic values provided in this paper will aid computational efforts, accelerate the optimization of computational models and further advance the potential application of UPCs in the reprocessing scheme of nuclear fuel and of POMs more widely.

Acknowledgements

This work was supported by the National Nuclear Security Administration, Department of Energy, under Award No. DE-NA0003763. This work was supported by LCs EPSRC grants (No. EP/J015156/1; EP/L023652/1; EP/I033459/1; EP/J015156/1; EP/K023004/1; and EP/L023652/1) and the ERC Advanced Grant (ERC-ADG, 670467 SMART-POM). The Material Characterization Facility of the Center for Sustainable Energy at Notre Dame provided thermogravimetric analysis instrumentation.

References

(1) Nyman, M.; Burns, P. C. A comprehensive comparison of transition-metal and actinyl polyoxometalates. Chem. Soc. Rev. 2012, 41 (22), 7354–7367.
(2) Lv, H. J.; Geletii, Y. V.; Zhao, C. C.; Vickers, J. W.; Zhu, G. B.; Luo, Z.; Song, J.; Lian, T. Q.; Musaev, D. G.; Hill, C. L. Polyoxometalate water oxidation catalysts and the production of green fuel. Chem. Soc. Rev. 2012, 41 (22), 7572–7589.
(3) Ji, Y. C.; Huang, L. J.; Hu, J.; Streb, C.; Song, Y. F. Polyoxometalate-functionalized nanocarbon materials for energy conversion, energy storage and sensor systems. Energy Environ. Sci. 2015, 8 (3), 776–789.
(4) Shiddiq, M.; Komijani, D.; Duan, Y.; Gaita-Ariño, A.; Coronado, E.; Hill, S. Enhancing coherence in molecular spin qubits via atomic clock transitions. Nature 2016, 531 (7594), 348–351.
(5) Herrmann, S.; Ritchie, C.; Streb, C. Polyoxometalate - conductive polymer composites for energy conversion, energy storage and nanostructured sensors. Dalton Trans. 2015, 44 (16), 7092– 7104.
(6) Wylie, E. M.; Peruski, K. M.; Prizio, S. E.; Bridges, A. N. A.; Rudisill, T. S.; Hobbs, D. T.; Phillip, W. A.; Burns, P. C. Processing used nuclear fuel with nanoscale control of uranium and ultrafiltration. J. Nucl. Mater. 2016, 473, 125–130.
(7) Wylie, E. M.; Peruski, K. M.; Weidman, J. L.; Phillip, W. A.; Burns, P. C. Ultrafiltration of Uranyl Peroxide Nanoclusters for the Separation of Uranium from Aqueous Solution. ACS Appl. Mater. Interfaces 2014, 6 (1), 473–479.
(8) Blanchard, F.; Ellart, M.; Rivenet, M.; Vigier, N.; Hablot, I.; Morel, B.; Grandjean, S.; Abraham, F. Neodymium uranyl peroxide synthesis by ion exchange on ammonium uranyl peroxide nanoclusters. Chem. Commun. 2016, 52 (20), 3947–3950.
(9) Li, H.; Shen, Y.; Yang, P.; Szymanowski, J. E. S.; Chen, J.; Gao, Y.; Burns, P. C.; Kortz, U.; Liu, T. Isotope and Hydrogen-Bond Effects on the Self-Assembly of Macroions in Dilute Solution. Chem. - Eur. J. 2019, 25 (71), 16288–16293.
(10) Burns, P. C. Complex minerals preserve natural geochemically important nanoscale metal oxide clusters. Acta Crystallogr., Sect. B: Struct. Sci., Cryst. Eng. Mater. 2020, 76, 512–513.
(11) Krivovichev, S. V. Polyoxometalate clusters in minerals: review and complexity analysis. Acta Crystallogr., Sect. B: Struct. Sci., Cryst. Eng. Mater. 2020, 76, 618–629.
(12) Friis, H.; Casey, W. H. Niobium is highly mobile as a polyoxometalate ion during natural weathering. Can. Mineral. 2018, 56 (6), 905–912.
(13) Hutin, M.; Long, D. L.; Cronin, L. Controlling the Molecular Assembly of Polyoxometalates from the Nano to the Micron Scale: Molecules to Materials. Isr. J. Chem. 2011, 51 (2), 205–214.
(14) Qiu, J.; Burns, P. C. Clusters of Actinides with Oxide, Peroxide, or Hydroxide Bridges. Chem. Rev. 2013, 113 (2), 1097–1120.
(15) Burns, P. C.; Nyman, M. Captivation with encapsulation: a dozen years of exploring uranyl peroxide capsules. Dalton Trans. 2018, 47 (17), 5916–5927.
(16) Proust, A.; Thouvenot, R.; Gouzerh, P. Functionalization of polyoxometalates: towards advanced applications in catalysis and materials science. Chem. Commun. 2008, No. 16, 1837–1852.
(17) Arteaga, A.; Zhang, L.; Hickam, S.; Dembowski, M.; Burns, P. C.; Nyman, M. Uranyl-Peroxide Capsule Self-Assembly in Slow Motion. Chem. - Eur. J. 2019, 25 (24), 6087–6091.

(18) Dembowski, M.; Colla, C. A.; Yu, P.; Qiu, J.; Szymanowski, J. E. S.; Casey, W. H.; Burns, P. C. The Propensity of Uranium-Peroxide Systems to Preserve Nanosized Assemblies. Inorg. Chem. 2017, 56 (16), 9602−9608.
(19) Xu, M.; Traustason, H.; Bo, F. D.; Hickam, S.; Chong, S.; Zhang, L.; Oliver, A. G.; Burns, P. C. Supramolecular Assembly of Geometrically Unstable Hybrid Organic-Inorganic Uranyl Peroxide Cage Clusters and Their Transformations. J. Am. Chem. Soc. 2019, 141 (32), 12780−12788.
(20) Xuan, W. M.; Pow, R.; Zheng, Q.; Watfa, N.; Long, D. L.; Cronin, L. Ligand-Directed Template Assembly for the Construction of Gigantic Molybdenum Blue Wheels. Angew. Chem., Int. Ed. 2019, 58 (32), 10867−10872.
(21) Xuan, W. M.; Pow, R.; Long, D. L.; Cronin, L. Exploring the Molecular Growth of Two Gigantic Half-Closed Polyoxometalate Clusters {Mo-180} and {Mo130Ce6}. Angew. Chem., Int. Ed. 2017, 56 (33), 9727−9731.
(22) Misra, A.; Kozma, K.; Streb, C.; Nyman, M. Beyond Charge Balance: Counter-Cations in Polyoxometalate Chemistry. Angew. Chem., Int. Ed. 2020, 59 (2), 596−612.
(23) Sures, D.; Segado, M.; Bo, C.; Nyman, M. Alkali-Driven Disassembly and Reassembly of Molecular Niobium Oxide in Water. J. Am. Chem. Soc. 2018, 140 (34), 10803−10813.
(24) Arteaga, A.; Ray, D.; Glass, E.; Martin, N. P.; Zakharov, L. N.; Gagliardi, L.; Nyman, M. The Role of the Organic Solvent Polarity in Isolating Uranyl Peroxide Capsule Fragments. Inorg. Chem. 2020, 59 (3), 1633−1641.
(25) Peruski, K. M.; Bernales, V.; Dembowski, M.; Lobeck, H. L.; Pellegrini, K. L.; Sigmon, G. E.; Hickam, S.; Wallace, C. M.; Szymanowski, J. E. S.; Balboni, E.; Gagliardi, L.; Burns, P. C. Uranyl Peroxide Cage Cluster Solubility in Water and the Role of the Electrical Double Layer. Inorg. Chem. 2017, 56 (3), 1333−1339.
(26) Flynn, S. L.; Szymanowski, J. E. S.; Gao, Y. Y.; Liu, T. B.; Burns, P. C.; Fein, J. B. Experimental measurements of U60 nanocluster stability in aqueous solution. Geochim. Cosmochim. Acta 2015, 156, 94−105.
(27) Dembowski, M.; Pilgrim, C. D.; Hickam, S.; Spano, T.; Hamlin, D.; Oliver, A. G.; Casey, W. H.; Burns, P. C. Dynamics of CationInduced Conformational Changes in Nanometer-Sized Uranyl Peroxide Clusters. Inorg. Chem. 2020, 59 (4), 2495−2502.
(28) Burns, P. C.; Kubatko, K. A.; Sigmon, G.; Fryer, B. J.; Gagnon, J. E.; Antonio, M. R.; Soderholm, L. Actinyl peroxide nanospheres. Angew. Chem., Int. Ed. 2005, 44 (14), 2135−2139.
(29) Hickam, S.; Aksenov, S. M.; Dembowski, M.; Perry, S. N.; Traustason, H.; Russell, M.; Burns, P. C. Complexity of Uranyl Peroxide Cluster Speciation from Alkali-Directed Oxidative Dissolution of Uranium Dioxide. Inorg. Chem. 2018, 57 (15), 9296− 9305.
(30) Falaise, C.; Nyman, M. The Key Role of U-28 in the Aqueous Self-Assembly of Uranyl Peroxide Nanocages. Chem. - Eur. J. 2016, 22 (41), 14678−14687.
(31) Sigmon, G. E.; Unruh, D. K.; Ling, J.; Weaver, B.; Ward, M.; Pressprich, L.; Simonetti, A.; Burns, P. C. Symmetry versus Minimal Pentagonal Adjacencies in Uranium-Based Polyoxometalate Fullerene Topologies. Angew. Chem., Int. Ed. 2009, 48 (15), 2737−2740.
(32) Sharifironizi, M.; Szymanowski, J. E. S.; Qiu, J.; Castillo, S.; Hickam, S.; Burns, P. C. Charge Density Influence on Enthalpy of Formation of Uranyl Peroxide Cage Cluster Salts. Inorg. Chem. 2018, 57 (18), 11456−11462.
(33) Tiferet, E.; Gil, A.; Bo, C.; Shvareva, T. Y.; Nyman, M.; Navrotsky, A. The Energy Landscape of Uranyl- Peroxide Species. Chem. - Eur. J. 2014, 20 (13), 3646−3651.
(34) Armstrong, C. R.; Nyman, M.; Shvareva, T.; Sigmon, G. E.; Burns, P. C.; Navrotsky, A. Uranyl peroxide enhanced nuclear fuel corrosion in seawater. Proc. Natl. Acad. Sci. U. S. A. 2012, 109 (6), 1874−1877.
(35) Long, D. L.; Burkholder, E.; Cronin, L. Polyoxometalate clusters, nanostructures and materials: From self assembly to designer materials and devices. Chem. Soc. Rev. 2007, 36 (1), 105−121.
(36) Traustason, H.; Aksenov, S. M.; Burns, P. C. The lithium-water configuration encapsulated by uranyl peroxide cage cluster U-24. CrystEngComm 2019, 21 (3), 390−393.
(37) Muller, A.; Krickemeyer, E.; Meyer, J.; Bogge, H.; Peters, F.; Plass, W.; Diemann, E.; Dillinger, S.; Nonnenbruch, F.; Randerath, M.; Menke, C. [Mo154(NO)14O420(OH)28(H2O)70] (25±5)- : A WaterSoluble Big Wheel with More than 700 Atoms and a Relative Molar Mass of About 24000. Angew. Chem., Int. Ed. Engl. 1995, 34 (19), 2122−2124.
(38) Muller, A.; Krickemeyer, E.; Bogge, H.; Schmidtmann, M.; Peters, F. Organizational forms of matter: An inorganic super fullerene and keplerate based on molybdenum oxide. Angew. Chem., Int. Ed. 1998, 37 (24), 3359−3363.

(39) Langmuir, D. Aqueous Environmental Geochemistry; PrenticeHall, Inc.: New Jersey, 1997.
(40) Forbes, T. Z.; Nyman, M.; Rodriguez, M. A.; Navrotsky, A. The energetics of lanthanum tantalate materials. J. Solid State Chem. 2010, 183 (11), 2516–2521.
(41) Kubatko, K. A. H.; Helean, K. B.; Navrotsky, A.; Burns, P. C. Stability of peroxide-containing uranyl minerals. Science 2003, 302 (5648), 1191–1193.
(42) Robbins, P. J.; Surman, A. J.; Thiel, J.; Long, D.-L.; Cronin, L. Use of ion-mobility mass spectrometry (IMS-MS) to map polyoxometalate Keplerate clusters and their supramolecular assemblies. Chem. Commun. 2013, 49 (19), 1909–1911.
(43) Xuan, W.; Pow, R.; Watfa, N.; Zheng, Q.; Surman, A. J.; Long, D.-L.; Cronin, L. Stereoselective Assembly of Gigantic Chiral Molybdenum Blue Wheels Using Lanthanide Ions and Amino Acids. J. Am. Chem. Soc. 2019, 141 (3), 1242–1250.
(44) Miro, P.; Pierrefixe, S.; Gicquel, M.; Gil, A.; Bo, C. On the Origin of the Cation Templated Self-Assembly of Uranyl-Peroxide Nanoclusters. J. Am. Chem. Soc. 2010, 132 (50), 17787–17794.
(45) Gao, Y. Y.; Haso, F.; Szymanowski, J. E. S.; Zhou, J.; Hu, L.; Burns, P. C.; Liu, T. B. Selective Permeability of Uranyl Peroxide Nanocages to Different Alkali Ions: Influences from Surface Pores and Hydration Shells. Chem. - Eur. J. 2015, 21 (51), 18785–18790.
(46) Kosova, D. A.; Druzhinina, A. I.; Tiflova, L. A.; Monayenkova, A. S.; Belyaeva, E. V.; Uspenskaya, I. A. Thermodynamic properties of ammonium sulfamate. J. Chem. Thermodyn. 2019, 132, 432–438.
(47) Thourey, J.; Bendaoud, S.; Perachon, G. Enthalpies of Dissolution of Ammonium Fluoride and Ammonium HydrogenFluoride in Water. J. Fluorine Chem. 1983, 23 (4), 331–338.
(48) Yin, P. C.; Li, D.; Liu, T. B. Solution behaviors and selfassembly of polyoxometalates as models of macroions and amphiphilic polyoxometalate-organic hybrids as novel surfactants. Chem. Soc. Rev. 2012, 41 (22), 7368–7383.
(49) Sigmon, G. E.; Burns, P. C. Rapid Self-Assembly of Uranyl Polyhedra into Crown Clusters. J. Am. Chem. Soc. 2011, 133 (24), 9137–9139.
(50) Sigmon, G. E.; Weaver, B.; Kubatko, K. A.; Burns, P. C. Crown and Bowl-Shaped Clusters of Uranyl Polyhedra. Inorg. Chem. 2009, 48 (23), 10907–10909.
(51) Qiu, J.; Ling, J.; Sui, A.; Szymanowski, J. E. S.; Simonetti, A.; Burns, P. C. Time-Resolved Self-Assembly of a Fullerene-Topology Core-Shell Cluster Containing 68 Uranyl Polyhedra. J. Am. Chem. Soc. 2012, 134 (3), 1810–1816.